Desalination and Water Treatment
www.deswater.com

doi: 10.1080/19443994.2015.1044919

57 (2016) 11685–11698
May

Taylor & Francis
Taylor & Francis Group

Influence of membrane, pH and water matrix properties on the retention of emerging contaminants by ultrafiltration and nanofiltration

Juan L. Acero*, F. Javier Benítez, Francisco J. Real, Elena Rodriguez

Chemical Engineering Department, Universidad de Extremadura, Badajoz 06006, Spain, Tel. +34924289384; Fax: +34924289385; emails: jlacero@unex.es (J.L. Acero), javben@unex.es (F. Javier Benítez), fjreal@unex.es (F.J. Real), elena@unex.es (E. Rodriguez)

Received 5 January 2015; Accepted 21 April 2015

ABSTRACT

The removal of five emerging contaminants (ECs) (1-H-benzotriazole, DEET, chlorophene, 3-methylindole and nortriptyline) dissolved in several water matrices by ultrafiltration and nanofiltration (NF) membranes has been investigated. Pore blocking and cake layer formation probably dominated at the beginning of filtration, whereas cake layer formation was likely the dominant fouling mechanism at later stages. The NF HL membrane was the most appropriate for the removal of the selected ECs, except for benzotriazole, which presented low retention. Therefore, the NF HL membrane is a feasible option for drinking water production and for the purification of not very contaminated secondary effluents for reuse.

Keywords: Ultrafiltration; Emerging contaminants; Retention coefficients; Water matrix properties

1. Introduction

In recent years, an increasing attention has been paid to a wide group of numerous chemical substances, including pharmaceutically active compounds, endocrine disrupting compounds and personal care products [1]. All of them are considered emerging contaminants (ECs), since they are still unregulated or in the process of being regulated. Wastewater treatment plant (WWTP) effluents are a major source of ECs in the environment, and they are found in wastewater effluents, surface water and treated drinking water [2–4]. Therefore, ECs constitute a potential risk for human health, since they can cause unexpected physiological consequences.

In general, their removal by conventional wastewater and drinking water processes has not been shown to be effective [5,6], and consequently, there is a need to investigate new technologies for their elimination. Due to this concern, different physical–chemical processes have been proposed as tertiary treatment of secondary effluents from municipal treatment plants, such as activated carbon adsorption [3,7], advanced oxidation by ozone and hydroxyl radicals [2] and photo-catalysis UV/TiO_2 [8]. More recently, membrane processes employing ultrafiltration (UF) and nanofiltration (NF) are increasingly used in wastewater reclamation and in drinking water to remove micropollutants as well as natural organic matter (NOM) [9–13]. Retention of organic micropollutants by UF membranes is attributed to adsorption on the membrane during the early stages of filtration or to interactions with the membrane fouling layer, and/or interactions with dissolved NOM in solution [14]. On the other hand, NF membranes remove organic solutes by three main mechanisms, i.e. size exclusion,

---

*Corresponding author.

electrostatic repulsion and adsorption [15–17]. The presence of NOM contributes to NF membrane fouling and may change the surface properties and therefore may affect the retention mechanism [18]. In addition, solute–solute interactions [19] and feed conditions (pH, ionic strength and temperature) [20] affect retention and membrane adsorption of the micropollutants. Similarly, the presence of cations can influence the interaction of compounds and NOM with each other as well as with the membrane surface [20–22]. Although some studies have investigated the removal of ECs in presence of NOM and cations, the complexity of fouling on retention mechanisms of ECs by UF and NF membranes needs further investigation.

This research is focused in the assessment of the specific elimination of a group of five frequently found ECs in water systems by means of UF and NF membranes. The ECs selected were the following: 1-H-benzotriazole (BZ), a well-known corrosion inhibitor for copper or silver material, widely used in cooling and hydraulic fluids, anti-freezing products, aircraft deicer and anti-ice fluid, and dishwasher detergents [23]; N,N-diethyl-m-toluamide or DEET (DT), an active compound in insect repellents [24]; chlorophene (CP), a widespread broad-spectrum antimicrobial pharmaceutical, used in hospitals and households for general cleaning and as active agent in disinfectant formulations [25]; 3-methylindole (ML), used as perfume and synthesizing anti-inflammatory drug, antibiotic, dye, plant growth hormone, herbicide, muscular relaxant, respiratory inhibitor and heart stimulant medicaments [26]; and the pharmaceutical nortriptyline HCl (NH), which belongs to the group of tricyclic antidepressants and is used in treatments against depression [27].

In the first stage of this work, the selected compounds were dissolved in ultrapure (UP) water and in the second stage in different water matrices, including synthetic and real waters. Several objectives were pursued: the study of the evolution of the permeate flux with filtration time and volume retention factors; the establishment of the effect of several operating parameters (pH, nature and molecular weight cut-off (MWCO) of the membranes) on the steady-state permeate flux; the evaluation of the partial contribution of the different membrane resistances; and the determination of retention coefficients and adsorbed mass for each EC, including the proposition of the main retention mechanisms. Finally, the influence of the water matrix properties (presence of NOM and cations) was also investigated, since the additional presence of humic acids and cations might affect the permeate flux and therefore modify the retention coefficients and mechanisms.

2. Materials and methods

2.1. Chemicals and water matrices

The five selected ECs were purchased from Sigma-Aldrich (Germany) and were of 99% purity or higher. Table 1 summarizes the selected compounds and their relevant physico-chemical properties related to the main removal mechanisms by membrane processes. Differences in hydrophobicity (expressed as log K_{ow}) and charge characteristics were chosen to enable assessment of the influence of hydrophobic interactions and charge on retention. The solutions used in this study were prepared by dissolving the ECs (1 μM of each) in UP water (from a Milli-Q system, Millipore Ibérica, Spain) or in synthetic water (SW) prepared from UP water buffered with 1 mM sodium bicarbonate and spiked with humic acids (Aldrich, 0–23 mg L^{-1}) as a surrogate NOM and calcium ions (0–1 mM). In addition, three real water matrices were used in order to reproduce realistic water treatment conditions: a surface water collected from the public reservoir "Peña del Aguila" (PA), located in the Extremadura Community, south-west of Spain; and two secondary effluents from WWTPs corresponding to the cities of Badajoz (BA) and La Albuera (LA), also in the Extremadura Community. These water samples were stored at 4°C until use, and its main quality parameters are compiled in Table 2.

Table 1
Physico-chemical properties of model compounds

ECs	Category	MW, g mol^{-1}	pK_a	Log k_{ow}
1-H-Benzotriazole	Anticorrosive	119.1	0.40/8.20	1.44
Nortriptyline HCl	Antidepressant	299.8	10.21	4.51
DEET	Insect repellent	191.3	0.67	2.18
3-Methylindole	Fragrance	131.3	–	2.60
Chlorophene	Biocide	218.7	9.81	4.18

Table 2
Characterization of the selected real water matrices

	PA	LA	BA
pH	7.2	8.1	8.5
Conductivity (μs cm^{-1})	68.6	538	546
$A_{254\ nm}$ (cm^{-1})	0.190	0.054	0.286
COD (mg O_2 L^{-1})	24	12.4	53
Alkalinity (mg $CaCO_3$ L^{-1})	30	335	325
TOC (mg L^{-1})	6.8	2.5	19.2
Total nitrogen (mg N L^{-1})	1.51	21.3	35.5
Total phosphorus (mg P L^{-1})	0.041	0.156	1.76

Note: COD: chemical oxygen demand; TOC: total organic carbon.

2.2. Experimental equipment and membranes

UF and NF experiments were conducted in a laboratory cross-flow mode filtration apparatus, supplied by CM-CELFA Membrantrenntechnik AG (Seewen, Switzerland), model P-28^{TM}. The equipment was constituted by a 500 mL pressurized storage vessel and a gear pump which fed the solution to the flat-sheet membrane module at the desired flow rates. The whole equipment is temperature controlled by means of a water stream at the desired temperature that circulated through an external jacket that surrounded the storage vessel. The transmembrane pressure (TMP) in the experiments was controlled by feeding nitrogen gas to the head of the storage vessel. The cumulative permeate volume was measured with a Mettler balance.

Several flat-sheet commercial membranes provided by GE Osmonics (Florida, USA) were used, all of them with an effective surface area of 28 cm^2. They were three UF membranes, denoted PW, PT and GK with MWCO of 20,000, 5,000 and 2,000 Da, respectively, and three NF membranes, denoted CK, DK and HL, with similar MWCOs, in the range 150–300 Da. Their main properties (material, MWCO and contact angle) are compiled in Table 3. More specifically, the GK membrane was made of thin film composite, with a cross-linked aromatic polyamide top layer, and the PT and PW membranes were of polyethersulfone. These three membranes are hydrophilic, specially the GK membrane with a lower value of contact angle. On the other hand, DK and HL membranes were made of thin film composite (polypyperazinamide skin layer on a polyester support), and the CK membrane was of cellulose acetate. According to the determined contact angles, the CK membrane is hydrophobic, while DK and HL are hydrophilic. A new membrane was used in each experiment, rinsed with UP water and compacted by filtering UP water during 3 h before starting the filtration experiment.

2.3. Filtration experiments

The filtration experiments were conducted in tangential cross-flow mode, and the operating method was batch concentration, in which the concentrate stream was flowed back to the feed tank. During each experiment, temperature (20°C), tangential velocity (1 m s^{-1}) and TMP (3 bar for UF and 20 bar for NF) remained constant. The experiments performed with UP water were buffered at the desired pH with phosphate buffer (10 mM).

A standard operating protocol was followed, which was constituted by three steps: firstly, the new membrane was rinsed with UP water, compacted, and the permeate flux (J_{wi}) was measured with the aim of determining the membrane pure water permeability (PWP), which represents a main characteristic of a membrane. PWP was determined as the ratio between J_{wi} and the TMP of the experiment, and the average values obtained for the different membranes tested are summarized in Table 3. In a next step, the filtration of the selected ECs dissolved in UP water, SW or real water matrices (300 mL feed water volume with initial concentration of ECs of 1 μM) took place. At regular time intervals, the permeate volume was measured with a balance in order to determine the permeate flux (J_v). Simultaneously, samples of this permeate stream

Table 3
Properties of target membranes (material, MWCO, pH range and salt rejection provided by manufacturer). PWP values were determined at 20°C

Membrane	Material	MWCO, Da	pH	$MgSO_4$ rejection, %	Contact angle°	PWP, L h^{-1} m^{-2} bar^{-1}
PW	PES	20,000	2–11		50 ± 3	141.4
PT	PES	5,000	2–11		53 ± 2	29.7 ± 1.5
GK	TF	2,000	2–11		44 ± 3	3.8
CK	CA	150–300	2–8	92	70 ± 3	2.1
DK	TF	150–300	2–11	98	31 ± 3	1.8
HL	TF	150–300	3–9	98	30 ± 3	10.2 ± 0.3

were retired in order to analyse the content of the selected pollutants, as well as the global quality parameters in the water matrices (chemical oxygen demand (COD), UV absorbance at 254 nm (A_{254}) and total organic carbon (TOC)). These experiments lasted until a volume reduction factor (VRF) of 3 was reached, collecting around 200 and 100 mL of permeate and concentrate, respectively. Once the filtration of ECs was finished, at the third step the feed tank was emptied and filled with UP water, and then, the membrane was rinsed by circulating UP water inside the membrane module in order to remove the cake layer formed on the membrane surface. The final pure water flux (J_{wf}) was then measured in order to determine the irreversible membrane fouling.

2.4. Analytical methods

The analytical methods for the characterization of the selected water matrices were followed according to the Standard Methods [28]. TOC was determined using a TOC analyser TOC-multi N/C 3100 (Analytik Jena). Absorbance at 254 nm was measured in spectrophotometer Unicam Helios Beta. Conductivity and pH were measured using a multiparameter instrument Hanna HI 255. COD, total nitrogen and total phosphorus were determined using Dr Lange kits. On the other hand, concentrations of the five selected ECs were assayed by HPLC in a Waters Chromatograph (Alliance 2695) equipped with a 2998 Photodiode Array Detector and a Phenomenex Gemini C18 column (5µm, 150 × 3 mm). The analysis was performed in gradient mode with acetonitrile and 25 mM acid formic, at a flow rate of 0.2 mL min^{-1}. Further details about the analytical method are given elsewhere [29]. The injection volume was 100 µL in all cases. Detection was made at 250 nm for BZ, NH and DT and at 280 nm for ML and CP.

2.5. Theoretical calculations

The permeate volume (V_p) was continuously collected for each experiment, and the permeate flux (J_w in the case of UP water or J_v in the aqueous solutions of ECs dissolved in UP water, SW or real water matrices) was determined using the following expression:

$$J_w \text{ or } J_v = \frac{\Delta V_p}{\Delta t \, A} \tag{1}$$

where ΔV_p represents the cumulative permeate volume difference, Δt is the time difference, and A is the membrane area.

The VRF is defined as the ratio between the feed volume (V_f) and the retentate volume ($V_r = V_f – V_p$) and was calculated using the following equation:

$$\text{VRF} = \frac{V_f}{V_r} \tag{2}$$

Regarding to the resistances to the permeate flux, the total hydraulic resistance (R_t) was evaluated from the permeate flux J_v, according to the general Darcy's law:

$$R_t = \frac{\text{TMP}}{\mu \, J_v} \tag{3}$$

where TMP is the TMP and μ is the viscosity of the solution. This R_t is the result of several resistances in series:

$$R_t = R_m + R_f = R_m + R_{if} + R_{ef} \tag{4}$$

where R_m is the intrinsic resistance of clean membrane and R_f is the fouling resistance with two components, the internal (R_{if}) and external (R_{ef}) fouling. These resistances were determined following the procedure described elsewhere [30].

One of the best parameters which provide the efficiency of a membrane in a filtration process is the retention coefficient, which was determined for the selected ECs by the equation:

$$R = \frac{C_f - C_p}{C_f} \cdot 100 \tag{5}$$

where C_f and C_p are the concentrations of each EC in the feed and permeate streams, respectively. Similarly, retention coefficients were evaluated for the water quality parameters selected in the present work. For the specific case of COD, this coefficient was defined by the expression:

$$R_{\text{COD}} = \frac{\text{COD}_f - \text{COD}_p}{\text{COD}_f} \cdot 100 \tag{6}$$

where COD_f and COD_p represent the COD in the feed and permeate streams, respectively. Similar equations were used for TOC (R_{TOC}) and UV absorbance at 254 nm (R_{A254}).

The adsorption of contaminants onto the membrane surface and into the membrane pores was evaluated in order to assess the contribution of this mechanism to the global retention of the solutes by the selected membranes and to establish the retention mechanism for each specific compound. For this purpose, the adsorption percentage (AP) was determined by the expression [31]:

$$\mathrm{AP} = \frac{(C_\mathrm{f}\ V_\mathrm{f}) - \lfloor (C_\mathrm{p}\ V_\mathrm{p}) + (C_\mathrm{r}\ V_\mathrm{r}) \rfloor}{C_\mathrm{f}\ V_\mathrm{f}} \cdot 100 \qquad (7)$$

where V_f, V_p and V_r are the feed, permeate and retentate volumes and C_f, C_p and C_r are the feed, permeate and retentate concentrations for each micropollutant.

3. Results and discussion

3.1. Permeate flux, membrane fouling and analysis of resistances

The filtration process of the selected ECs dissolved together in UP water was performed using the UF and NF membranes already described and by varying some operating conditions: characteristics of the membranes (MWCO, material, etc.) and pH. The experiments performed and the values of the operating conditions are summarized in Table 4. In addition, some experiments were carried out with the ECs dissolved in SW and in the selected water matrices and subjected to both UF with the PT membrane and NF with the HL membrane. The criteria for selecting these PT and HL membranes were their better behaviour in terms of permeate flux, membrane fouling and retention of ECs within the investigated UF and NF membranes, respectively, as will be discussed later. These experiments are summarized in Table 4 as well.

The evolution of J_v with VRF in some experiments performed with UP water (UPUF-3 and UPNF-3), SW (SWUF-2 and SWNF-2) and BA water (BAUF and BANF) is shown in Fig. 1. When UP water was used, there was an initial decrease in J_v (5–15% of J_wi) with the increase of VRF, and later, after a specific time, the flux remained almost constant. However, J_v decrease was more pronounced when synthetic or real waters were employed, and the time required to reach an almost constant value was higher than with UP water. The decay of J_v is a consequence of membrane fouling, which can be due to different causes, such as polarization concentration, cake layer formation, pore blocking or adsorption of solutes onto the membrane [32,33]. According to the shape of J_v and results found in

Table 4
Filtration experiments performed with ECs dissolved in different water matrices (UP water, SW and real water matrices (PA, LA, and BA)): operating conditions, steady-state permeate flux (J_vss), flux decay ($J_\mathrm{vss}/J_\mathrm{wi}$) and flux recovery ($J_\mathrm{wf}/J_\mathrm{wi}$)

Experiments	Membrane	TMP, bar	pH	TOC, mg L^{-1}	Ca^{2+}, mM	J_vss, L h^{-1} m^{-2}	$J_\mathrm{vss}/J_\mathrm{wi}$	$J_\mathrm{wf}/J_\mathrm{wi}$
UPUF-1	PW	3	6	–	–	377.6	0.87	0.98
UPUF-2	GK	3	5.8	–	–	10.1	0.87	0.96
UPUF-3	PT	3	5.5	–	–	87.3	0.97	0.98
UPUF-4	PT	3	7	–	–	87.8	0.95	0.98
UPUF-5	PT	3	8.5	–	–	82.8	0.93	0.99
UPUF-6	PT	3	10	–	–	83.9	0.92	0.98
UPNF-1	DK	20	5.5	–	–	30.5	0.85	0.88
UPNF-2	CK	20	5.7	–	–	40.1	0.98	0.98
UPNF-3	HL	20	5.5	–	–	188.2	0.96	0.98
UPNF-4	HL	20	7	–	–	187.1	0.91	0.99
UPNF-5	HL	20	8.5	–	–	171.3	0.84	0.98
UPNF-6	HL	20	10	–	–	167.7	0.84	0.99
SWUF-1	PT	3	7.2	12	–	79.5	0.86	0.97
SWUF-2	PT	3	7.3	12	1	70.3	0.79	0.88
SWUF-3	PT	3	7.3	23	1	67.1	0.73	0.81
SWNF-1	HL	20	7.3	12	–	155.8	0.82	0.98
SWNF-2	HL	20	7.3	12	1	19.0	0.10	0.91
SWNF-3	HL	20	7.4	23	1	18.9	0.10	0.79
PAUF	PT	3	7.2	6.8	–	75.2	0.96	0.98
LAUF	PT	3	8.1	2.6	–	84.5	0.95	0.98
BAUF	PT	3	8.6	19.0	–	69.8	0.74	0.85
PANF	HL	20	7.2	6.8	–	167.3	0.84	0.98
LANF	HL	20	8.1	2.3	–	153.6	0.80	0.97
BANF	HL	20	8.5	19.3	–	121.5	0.62	0.89

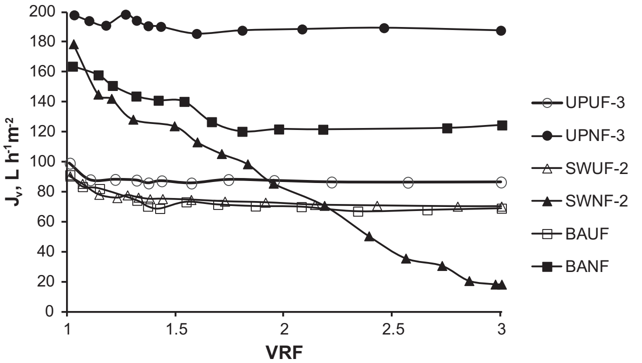

Fig. 1. Evolution of the permeate flux with VRF during the filtration of micropollutants dissolved in UP water (Expts. UPUF-3 and UPNF-3), SW (Expts. SWUF-2 and SWNF-2) and secondary effluent BA (Expts. BAUF and BANF). Experimental conditions are detailed in Table 4.

previous studies [32–34], pore blocking and cake layer formation probably dominated at the beginning of filtration, whereas cake layer formation was likely the dominant fouling mechanism at later stages. Polarization concentration could also contribute to membrane fouling, specially in experiments performed with UP water with very low foulant concentration. The almost constant permeate flux can be considered as the steady-state permeate flux (J_{vss}). Table 4 compiles the values of J_{vss} as well as the ratio $J_{\mathrm{vss}}/J_{\mathrm{wi}}$ (ratio between the steady-state permeate flux for the solution containing the ECs and that corresponding to the filtration of UP water without solutes). Finally, the values of $J_{\mathrm{wf}}/J_{\mathrm{wi}}$ were determined in order to evaluate the membrane flux recovery after washing with pure water, thus removing the external fouling. These values are also reported in Table 4 and provide an idea of the internal membrane fouling.

The values of J_{vss} are affected by the characteristics of the membranes (MWCO, material, etc.), pH and water matrix. With respect to the influence of the characteristics of the UF membranes, and although these membranes were different in materials, an influence of MWCO on J_{vss} can be deduced from the UF experiments compiled in Table 4 (Expts. UPUF-1 to UPUF-3). Thus, J_{vss} values were 10.1, 87.3, and 377.6 L h^{-1} m^{-2} for the membranes GK, PT and PW (MWCOs of 2, 5 and 20 kDa, respectively), being this increase of the permeate flux likely due to the MWCO increase. On the contrary, in the NF process no conclusion could be drawn on the effect of the MWCO (Expts. UPNF-1 to UPNF-3), since the three membranes present similar pore sizes (in the range 150–300 Da). Nevertheless, a much higher permeate flux was obtained for the HL membrane, while the CK and DK membranes presented lower values, differences that can be attributed to the different nature of these membranes. Specifically, this sequence agrees with the results previously reported for the PWP of the membranes (see Table 3), with a significant higher value for the HL membrane and similar lower values for the DK and CK membranes. The best results for permeate flux, membrane fouling and also for ECs retention (see below) were obtained for the UF membrane PT and the NF membrane HL. As a consequence, the remaining experiments performed at different pH and with several water matrices were carried out with these membranes.

The influence of pH on the values of J_{vss} as well as on the ratio $J_{\mathrm{vss}}/J_{\mathrm{wi}}$ is slightly negative. As can be observed in Table 4, a pH increase led to a decrease in the values of J_{vss} and an increase of the membrane fouling. An explanation for these results could be that a higher pH values, the negative zeta potential increase promotes stronger electrostatic interaction between dissociated functional groups of membrane material causing a pore constriction [35,36]. Additional solute–membrane interactions could also be responsible for the fouling increase, as well as an increase of the osmotic pressure near the membrane surface [37].

The influence of the water matrix on J_{vss} can also be deduced from the results summarized in Table 4 as well as from Fig. 1. Thus, the permeate fluxes obtained with UP water at pH 7 (87.8 and 187.1 L h^{-1} m^{-2} for PT and HL membranes, respectively) were higher than those obtained with the different water matrices in similar experiments, especially in the NF process, where the flux decrease was more pronounced.

As pointed out above, the decrease in the permeate flux is a consequence of polarization concentration, pore blocking and formation of a cake layer on the membrane surface as well as adsorption of species (NOM and ions) onto the membrane. Consequently, a decrease of the effective pore size is caused, which leads to a decrease of the water flux. It can be appreciated in the experiments performed with SWs that the presence of NOM led to a further decrease of the permeate flux as well as to a decrease of the ratio $J_{\mathrm{vss}}/J_{\mathrm{wi}}$. Furthermore, this decrease of the water flux was more pronounce in presence of both NOM and calcium ions. Certain compounds present in the NOM, mainly humic acids, are known to be hydrophobic and therefore might be adsorb on the membrane due to hydrophobic interactions, being one of the major causes of NF fouling. Pore blocking can be caused by molecules with a size that is similar to the size of an important fraction of the pores. Such type of molecules can block the membrane pores efficiently, and thus, the pores become unavailable for further filtration [38]. While internal pore adsorption is irreversible, pore blocking is partly reversed by backwashing [39]. Similarly, calcium ions are adsorbed onto the membrane surface and reduce its negative charge, which leads to a reduction of the membrane permeability and an increment of membrane-NOM interactions [35]. In cake layer formation, foulants deposit on the particles that already block the pores and result in cake formation [15]. At the same time, the formation of calcium complexes of humic acids could also contribute to cake layer formation. For these reasons, the extent of the membrane fouling was more important in the presence of both humic acids and calcium ions. Under these conditions, the main fouling mechanisms are an initial pore blocking stage (rapid fouling) followed by cake layer formation (slow fouling) [15]. Furthermore, membrane fouling was lower in the case of the UF membrane PT with a MWCO of 5 kDa, since fouling of UF membranes in presence of NOM is more important for those membranes of higher MWCO [14]. The important fouling of the HL membrane in presence of NOM and Ca^{2+} is mainly due to cake layer formation, since this fouling is mostly reversible and could be removed by rinsing with UP water, as can be deduced from the values of J_{wf}/J_{wi} summarized in Table 4.

Additionally, among the real waters investigated, the trend observed for J_{vss} and J_{vss}/J_{wi} was the following: PA ≈ LA > BA. The higher content of NOM in the secondary effluent BA (values of UV absorbance, TOC and DOC in Table 2) led to lower J_{vss} values due to the reasons given above. On the other hand, the results obtained for the reservoir water PA and the secondary effluent LA are rather similar. Compared to PA water, LA presents less NOM but higher inorganic matter content (from the values of conductivity and alkalinity summarized in Table 2). Although a limited membrane fouling could be expected from the low NOM content in LA secondary effluent, the presence of cations could enhance the formation of complexes with NOM and thus increase membrane fouling as mentioned above.

The permeate flux decline discussed is a consequence of the resistances found by the solutions to pass through the membranes during the filtration processes. Then, this decline can be analysed by means of the resistance in series model (Eqs. (3) and (4)). The values obtained for these resistances in all the experiments are summarized in Table 5, which also shows the partial contribution of the fouling resistance to the total resistance, represented by the ratio $(R_f/R_t) \times 100$.

In the experiments performed with UP water, R_f was much smaller than R_m for the different membranes tested, which confirms that the membrane fouling is low in these experiments performed with ECs dissolved in UP water. However, in the experiments carried out with synthetic and real waters, a significant increase was appreciated for the partial contribution of R_f–R_t, specially for the NF process. It should be noted that $R_f > R_m$ in the NF experiments performed with SW containing NOM and Ca^{2+}.

When the ECs were dissolved in UP water, the values of R_f were higher in the NF process than in the UF process, which indicates that NF membranes were more sensitive to fouling. Moreover, greater flux decrease values were obtained in the UF membranes with lower MWCO: thus, the GK membrane (2 kDa) presented the highest value of R_f within UF membranes. Although the MWCO of the selected NF membranes was similar, the HL membrane presented the lowest values of fouling resistance. With respect to the contribution of internal and external components to the total fouling, R_{ef} was higher than R_{if} for the selected UF membranes and also for the NF HL membrane. These results indicate that polarization concentration and cake layer formation contribute to a higher extent to fouling that pore blocking and contaminants adsorption onto the membrane, especially in the case of the hydrophilic membrane HL. However, R_{if} was higher than R_{ef} for the NF membranes CK and DK, which can be explained by the higher contribution of pore blocking rather than adsorption, since the APs are similar for the three NF membranes.

The pH influence on membrane fouling is negative, specially for the HL membrane (Expts. UPNF-3 to UPNF-6 in Table 5). This higher membrane fouling at greater pH is due to the increment of the external fouling, and therefore, the formation of the cake layer is favoured at high pH. These results can be explained by the reduction of the pore size and also by the enhanced solute–membrane interactions at high pH [36,37].

During the filtration of SWs, the additional presence of humic acids and calcium ions also increased R_t and R_f due to the adsorption of NOM and Ca^{2+} onto the membrane as well as to the formation of calcium complexes of humic acids as explained above. Thus, the initial concentration of humic acids as well as the additional presence calcium ions led to a moderate increase of R_{if}. Nevertheless, the highest increment for the different resistances was obtained for R_{ef} in the case of the NF HL membrane (Expts. SWNF-2 and SWNF-3), which is due to the cake layer formation enhancement in presence of both humic acids and Ca^{2+}. These results corroborate that cake layer formation is the dominant fouling mechanism for the NF membrane in presence of NOM-Ca complexes.

Table 5
Resistances obtained in the filtration of ECs dissolved in different water matrices at VRF = 3. Experimental conditions are shown in Table 4

Experimental	Membrane	$R_m \times 10^{-13}$, m^{-1}	$R_t \times 10^{-13}$, m^{-1}	$R_f \times 10^{-13}$, m^{-1}	$R_{ef} \times 10^{-13}$, m^{-1}	$R_{if} \times 10^{-13}$, m^{-1}	$(R_f/R_t) \times 100$, %
UPUF-1	PW	0.25	0.29	0.04	0.03	0.01	11.2
UPUF-2	GK	9.45	10.7	1.21	0.81	0.40	11.4
UPUF-3	PT	1.21	1.27	0.06	0.03	0.03	4.7
UPUF-4	PT	1.16	1.23	0.07	0.04	0.03	5.3
UPUF-5	PT	1.23	1.30	0.07	0.06	0.01	5.4
UPUF-6	PT	1.18	1.29	0.11	0.08	0.03	8.2
UPNF-1	DK	20.1	23.6	3.51	0.75	2.76	14.9
UPNF-2	CK	16.8	17.9	1.14	0.27	0.87	6.3
UPNF-3	HL	3.65	3.83	0.18	0.09	0.09	4.5
UPNF-4	HL	3.51	3.85	0.34	0.30	0.04	8.8
UPNF-5	HL	3.54	4.20	0.66	0.59	0.07	15.7
UPNF-6	HL	3.60	4.30	0.70	0.69	0.01	16.2
SWUF-1	PT	1.16	1.35	0.19	0.16	0.03	14.3
SWUF-2	PT	1.21	1.54	0.33	0.17	0.16	21.4
SWUF-3	PT	1.18	1.61	0.43	0.16	0.27	26.6
SWNF-1	HL	3.80	4.62	0.82	0.72	0.10	17.7
SWNF-2	HL	3.71	37.8	34.1	33.7	0.35	90.2
SWNF-3	HL	3.64	37.9	34.3	33.3	0.97	90.4
PAUF	PT	1.23	1.43	0.14	0.08	0.06	9.8
LAUF	PT	1.21	1.27	0.06	0.04	0.02	5.0
BAUF	PT	1.14	1.55	0.41	0.21	0.20	26.2
PANF	HL	3.63	4.30	0.67	0.58	0.09	15.6
LANF	HL	3.74	4.69	0.95	0.83	0.12	20.3
BANF	HL	3.49	5.86	2.37	1.65	0.72	40.4

With respect to the filtration of surface water and secondary effluents, the main increase in the values of R_f with respect to UP water filtration was obtained for the secondary effluent from BA, which is the most contaminated within the selected real water matrices. As can be observed in Table 5, both R_{if} and R_{ef} were higher for real waters than for UP water, which can be explained by the contribution of the different fouling mechanisms commented above (adsorption, pore blocking and cake layer formation) in presence of organic and inorganic matter (specially for the secondary effluent BA).

3.2. Retention and adsorption of ECs

The retention coefficients relate the concentration of a specific substance in the permeate stream with its concentration in the feed stream and were determined using Eq. (5). In general, R coefficients decreased slightly with the increase in VRF, and consequently with processing time. This decay is representative of filtration processes in batch concentration mode. In effect, the increase of VRF or water recovery leads to an increase of the concentration of ECs in the feed solution which facilitates their transport through the membrane.

The values of the retention coefficients of the ECs at steady-state conditions (VRF = 3) in all the UF and NF experiments carried out cover a wide range, because there are several membrane characteristics and solute properties that affect the retention (MW, molecular size, pK_a, log K_{ow}, dipole moment, etc.) by different mechanisms (adsorption, steric hindrance and electrostatic repulsion) [31]. In general terms, the retention of ECs by NF membranes was slightly higher than by UF membranes, as can be observed in Fig. 2, which represents the R coefficients for the selected ECs in experiments carried out with the six membranes tested (Expts. UPUF-1 to UPUF-3 and UPNF-1 to UPNF-3). The highest retentions were obtained with the UF PT membrane and with the NF HL membrane, and therefore, these membranes were selected for the experiments performed with synthetic and real waters.

The retention coefficients obtained for the selected ECs in the experiments performed with the UF

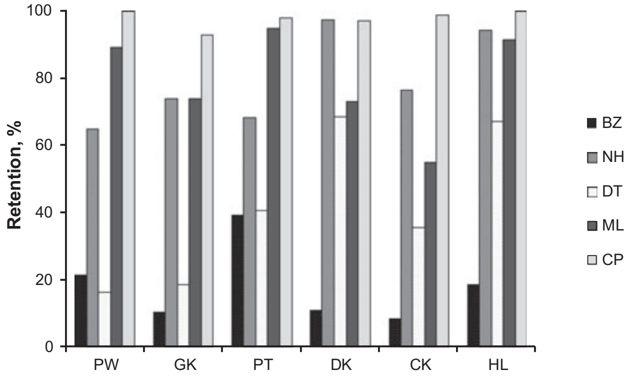

Fig. 2. Influence of the MWCO and nature of some UF (PW, GK, and PT) and NF (DK, CK, and HL) membranes on the retention of emerging compounds at VRF = 3 (Expts. UPUF-1 to UPUF-3 and UPNF-1 to UPNF-3 in Table 4).

membranes followed the sequence CP > ML > NH > DT > BZ (Fig. 2). According to these results, adsorption should be the main mechanism responsible for retention of ECs by UF membranes rather than size exclusion, since the MWCO of these membranes is much higher than the molecular weight of the selected pollutants. Thus, the highest values of retention coefficients with UF membranes were obtained for CP, which is a hydrophobic compound according to the values of log K_{ow} summarized in Table 1. Although NH is also a hydrophobic compound (log $K_{ow} = 4.51$), at acidic pH is partially protonated ($pK_a = 10.21$). The hydrophobicity of ionizable compounds can be determined as log $D = \log K_{ow}$—log $(1 + 10(pK_a\text{-}pH))$, being the value for NH of 1.40 at pH 7. Therefore, the hydrophobic character of NH decreases at lower pH, and thus, its adsorption is hindered. BZ presents the lowest MW (119.1 g mol^{-1}) and is the most hydrophilic compound and therefore adsorbed only partially onto the membranes, so that its retention is rather low. However, the retentions obtained with NF membranes followed the trend: CP > NH > ML > DT > BZ (Fig. 2). Therefore, other mechanisms such as size exclusion must also contribute efficiently to the retention of ECs by NF membranes. Thus, the retention coefficients obtained for NH, the EC with the highest MW (299.8 g mol^{-1}), were higher than those of ML. At the same time, the retention of BZ was lower with NF membranes (MWCO of 150–300 Da) than with UF membranes, since this contaminant has a MW lower than the MWCO of the selected NF membranes and is hardly adsorbed on NF membranes. In addition, the CK membrane provided lower retentions than DK and HL membranes, which can be due to its higher pore size [40]. Therefore, retention of ECs by NF membranes is controlled by a combination of size exclusion, and electrostatic repulsion specially when pH > pK_a [15], and only partially by adsorption.

The APs of the selected compounds on UF and NF membranes determined by Eq. (7) are summarized in Table 6. In most of the experiments, the values of AP followed the sequence CP > ML > NH > DT > BZ, accordingly with the hydrophobic character of selected ECs, since adsorption is strongly correlated with log K_{ow} [21]. Within the UF membranes, the highest values of AP were obtained for the PT membrane, which is the most hydrophobic membrane according to the values of contact angle detailed in Table 3. One could expect higher values of AP for the hydrophobic NF membrane CK (contact angle of 70°). However, the values of AP are very similar to those of the hydrophilic NF membranes HL and DK, which can be explained by the higher pore size of the CK membrane [40] or by the fact that adsorption is not the

Table 6
AP (AP, %) of ECs in filtration experiments performed with UP water at VRF = 3. Experimental conditions in Table 4.

Experimental	Membrane	pH	BZ	NH	DT	ML	CP
UPUF-1	PW	6	16.9	50.3	13.8	65.2	80.9
UPUF-2	GK	5.8	10.6	64.5	15.1	60.9	82.9
UPUF-3	PT	5.5	31.5	60.2	30.2	80.1	88.9
UPUF-4	PT	7.0	35.5	67.6	37.3	81.0	88.2
UPUF-5	PT	8.5	28.1	71.8	34.9	78.4	86.6
UPUF-6	PT	10	22.4	88.5	37.3	81.3	82.2
UPNF-1	DK	5.5	7.9	70.9	17.6	59.1	84.1
UPNF-2	CK	5.7	8.2	71.4	19.0	44.9	86.6
UPNF-3	HL	5.5	18.8	45.9	19.3	72.3	84.9
UPNF-4	HL	7.0	19.2	52.8	20.0	78.4	83.5
UPNF-5	HL	8.5	18.4	57.0	19.5	75.5	83.1
UPNF-6	HL	10	11.8	65.9	20.5	78.2	69.4

dominant mechanism for micropollutant retention with NF membranes. In addition, the values of AP for the NF membranes were lower than their corresponding values of *R* and also lower than the values of AP for the UF membranes. These results confirm that adsorption is not the main mechanism for ECs retention with NF membranes.

Figs. 3 and 4 depict the values of R and AP, respectively, obtained for the selected ECs in experiments carried out with UP water at different pH. The variation of pH exerted slightly different influence on the retention of ECs in the UF process with the PT membrane (Expts. UPUF-3 to UPUF-6) and in the NF process with the HL membrane (Expts. UPNF-3 to UPNF-6), as can be appreciated in Fig. 3. Thus, the retention of BZ ($pK_a = 8.20$) decreased at high pH (Fig. 3(a)), which is due to the hindered adsorption of the anionic species. However, the retention of BZ increased with pH in the case of the NF membrane HL (Fig. 3(b)), which can be explained by the contribution of the electrostatic repulsion mechanism to the global retention of BZ. CP, which is also negatively charged at high pH ($pK_a = 9.81$), was almost completely rejected at any pH, and therefore, the influence of pH was not appreciable. At the same time, the values of AP for BZ and CP decreased at high pH, as can be appreciated in Fig. 4(a) and (b) for PT and HL membranes, respectively. As pH increases, log *D* decreases for BZ and CP, being their adsorption on the membranes hindered. On the other hand, the values of retention and AP for NH increased with pH, as could be expected from the deprotonation of this compound at high pH ($pK_a = 10.21$), being the neutral species more easily adsorbed. Finally, the values of R and AP for DT and ML remained fairly constants with the variation of pH, as corresponds to non ionic compounds in the investigated pH range. These results can be justified if adsorption is the main mechanism responsible for micropollutants retention by UF membranes, being the adsorption of neutral species more favourable [31]. Instead, for the NF HL membrane, in addition to size exclusion and partially to adsorption, electrostatic repulsion must contribute efficiently to the retention of negative species at high pH, while the retention of neutral compounds remains fairly independent on pH.

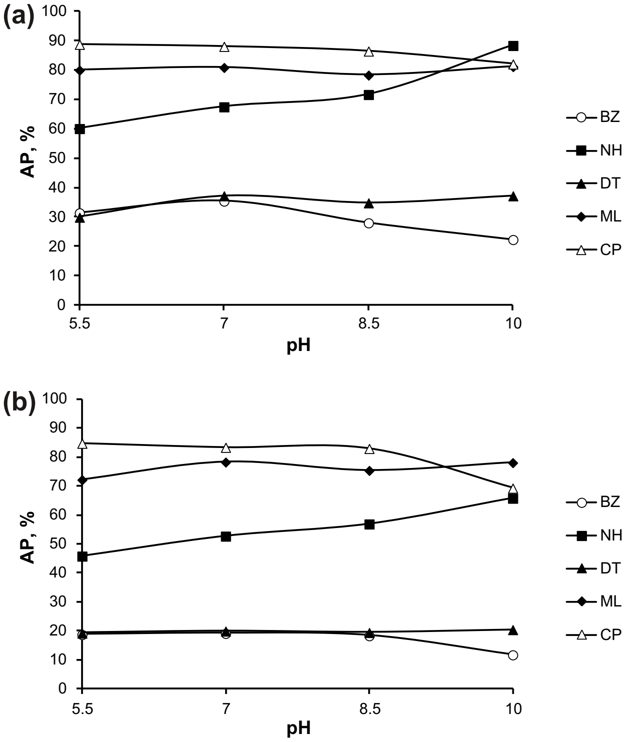

Fig. 4. AP for each selected micropollutant obtained in experiments performed at different pH with (a) the UF PT membrane (Expts. UPUF-3 to UPUF-6) and (b) the NF HL membrane (Expts. UPNF-3 to UPNF-6). Experimental conditions are detailed in Table 4.

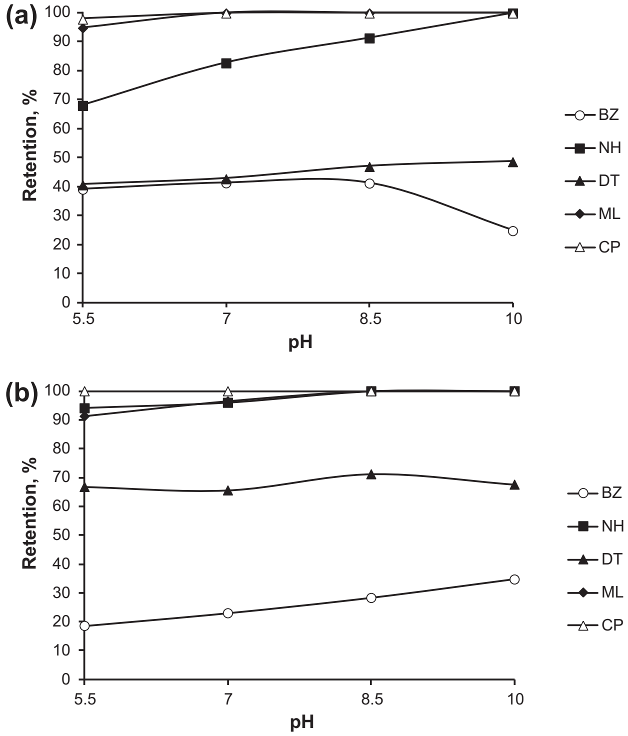

Fig. 3. Retention of selected micropollutants obtained in experiments performed at different pH with (a) the UF PT membrane (Expts. UPUF-3 to UPUF-6) and (b) the NF HL membrane (Expts. UPNF-3 to UPNF-6). Experimental conditions are detailed in Table 4.

In order to establish the influence of the water matrix constituents on the retention of the investigated ECs, the results obtained in the filtration of SWs and real waters in experiments performed with the UF PT and the NF HL membrane are depicted in Fig. 5(a) and (b), respectively. Compared to the results obtained with UP water, the presence of NOM (Expts. SWUF-1 and SWNF-1) slightly enhanced the retention of the selected ECs. However, the additional presence of calcium ions (Expts. SWUF-2 and SWNF-2) exerted a negative effect on the retention of these contaminants with UF and NF membranes. Finally, a slight increase of retentions was observed when the concentration of humic acids was increased from 12 to 23 g L^{-1} in presence of the same amount of Ca^{2+} (1 mM, Expts. SWUF-3 and SWNF-3). Contaminants removal enhancement in presence of NOM might be due to the formation of macromolecular complexes with NOM functional groups (size exclusion and adsorption) and/or increased level of charge density induced by NOM in "pseudo-complexes" (electrostatic repulsion) [13,21]. In addition, the fouling layer may act as a more selective secondary membrane capable of retaining larger molecular weight and hydrophobic micropollutants [12]. However, the additional presence of divalent cations transform the flexible, linear humic molecules to a rigid, compact and coiled conformation by forming metal-humic complexes and reducing the negative charges of humic carboxylic functional groups [41]. Therefore, increases in divalent cation concentration cause NOM macromolecular conformation changes and may alter the distribution of sites for compound association, resulting in a reduction of compound-NOM complexation [20], and as a consequence, ECs retention is hindered.

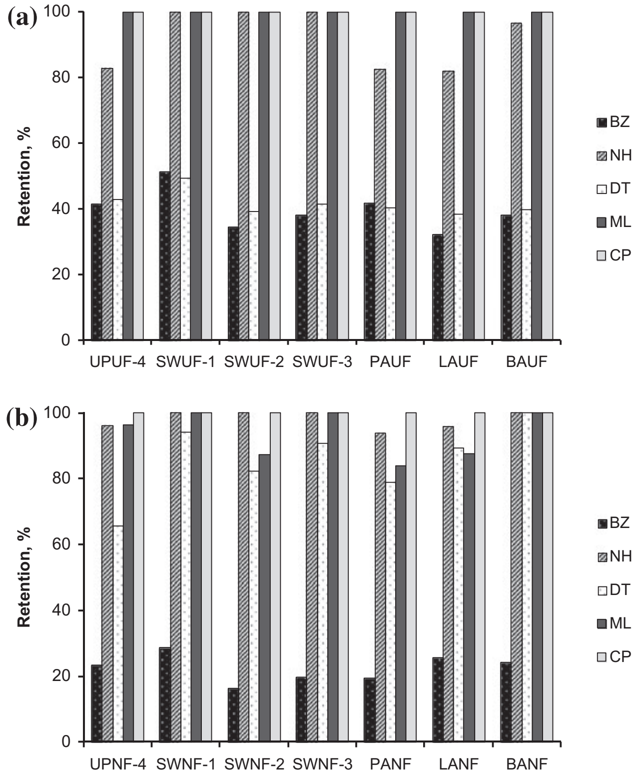

Fig. 5. Influence of water matrix composition on retention of selected micropollutants in experiments performed with (a) the UF PT membrane and (b) the NF HL membrane. Experimental conditions are detailed in Table 4.

Finally, by considering the nature of the real water matrices, the retention coefficients for a specific compound reveal that slightly higher retentions were obtained in the secondary effluent BA, while lower values were obtained in the reservoir water PA and the secondary effluent LA (Fig. 5(a) and (b)). These results can be explained since the secondary effluent BA, with higher NOM content, induces higher membrane fouling in comparison to the reservoir water PA and the secondary effluent LA, with lower NOM content, and this membrane fouling decreases the pore size and increases the ECs retention. Additionally, contaminants interactions with the organic matter present in the water matrix itself might increase ECs retention as commented above. Although the initial concentration of contaminants used in the experiments was higher than that found in environmental water samples, the results (fouling mechanism and retention of ECS) from experiments performed with lower concentration of contaminants are not expected to be different.

In addition to the retention coefficients for the specific compounds, the effectiveness of the filtration processes for the elimination of the organic matter present in different water matrices can be also evaluated by the retention coefficients referred to the water quality parameters selected in this work: absorbance at 254 nm (A_{254}), COD and TOC. These coefficients were evaluated by means of Eq. (6), and the values obtained for VRF = 3 are summarized in Table 7. In general terms, lower removals were obtained in the UF process (in the range 39–91% for A_{254}, 4–72% for COD and 7–82% for TOC) than in the NF process (in the range 67–99% for A_{254}, 45–81% for COD and 72–91% for TOC), as could be expected for membranes with much lower MWCO. Therefore, size exclusion must be the main retention mechanism for high MW compounds. In addition, the retention of these parameters followed the sequence: $A_{254} > TOC > COD$. Absorbance at 254 nm retention was higher than COD or TOC retention since UV absorbance at 254 nm is mainly due to aromatic/hydrophobic compounds that

Table 7
Retention coefficients obtained for several quality parameters in the filtration of synthetic and real waters with the UF PT and NF HL membranes (VRF = 3)

Experimental	$R_{A,254}$, %	R_{COD}, %	R_{TOC}, %
SWUF-1	91.1	71.7	82.4
SWUF-2	87.1	63.4	74.5
SWUF-3	87.3	71.9	80.7
SWNF-1	98.8	77.8	91.4
SWNF-2	96.7	74.8	90.6
SWNF-3	99.1	81.3	91.2
PAUF	68.4	48.7	55.4
LAUF	39.2	3.9	7.1
BAUF	50.9	44.4	48.2
PANF	91.0	76.4	83.2
LANF	67.3	45.2	72.7
BANF	90.4	74.1	86.5

might be absorbed on the membranes, whereas COD or TOC measure the concentration of overall compounds.

The presence of humic acids and calcium ions in SWs led to a high retention of the selected parameters (Table 7) due to the formation of complexes and adsorption on the membranes as commented above. COD and TOC retention was slightly lower when Ca^{2+} was present in addition to humic acids (compare Expts. SWUF-2 and SWUF-1 or Expts. SWNF-2 and SWNF-1) due to the different configuration of metal-humic complexes and the reduced negative charges of humic carboxylic functional groups. With respect to the real water matrices, the lowest values of retention coefficients for the investigated water quality parameters were obtained for the secondary effluent LA, which is probably due to its low content of organic matter. In addition, the retention of COD and TOC in LA water with the UF PT membrane was very low, which is an indication that the NOM present in this secondary effluent has a MW not very high.

4. Conclusions

According to the results obtained in the UF and NF experiments of five ECs, flux decline was higher when the ECs were dissolved in synthetic and real water matrices as a consequence of membrane fouling. The pH effect on the permeate flux was negative due to stronger electrostatic interaction between dissociated functional groups of membrane material causing a pore constriction. Among fouling mechanisms, pore blocking and cake layer formation probably dominated at the beginning of filtration, whereas cake layer formation was likely the dominant fouling mechanism at later stages. The important fouling of the NF HL membrane in presence of NOM and Ca^{2+} is mainly due to cake layer formation, since this fouling is mostly external and reversible.

Under a point of view of the retention coefficients, the NF HL membrane was the most appropriate for the removal of the selected ECs from the waters tested, excepting benzotriazole. The effect of pH on the retention of negatively charged compounds was negative for UF membranes (due to the decrease of adsorption at high pH) and slightly positive for NF membranes (because of electrostatic repulsion at high pH). While adsorption is the main retention mechanism for UF membranes, size exclusion and electrostatic repulsion of negative species at high pH are mainly responsible for micropollutant retention by NF membranes. In addition, the presence of NOM increased retention likely due to micropollutants–humic acids interactions. However, the additional presence of Ca^{2+} decreased the contaminant removal probably due to reduced humic acids interaction sites.

With respect to the selected membranes, and taking into account permeate fluxes and retentions, PT and HL membranes, among UF and NF membranes, respectively, provided the best results for the retention of micropollutants at high permeate fluxes and with lower fouling. Additionally, the NF HL membrane also provided high retentions for COD and TOC (around 80%) and aromatic compounds (around 90%). It must be noticed that the significant removal of NOM, especially hydrophobic and aromatic compounds, reduces the disinfection by-products formation potential in the final water. Therefore, the HL membrane is adequate for natural water treatment to produce drinking water and for the purification of not very contaminated secondary effluents for reuse.

Acknowledgments

Authors gratefully acknowledge the financial support from the MINECO of Spain and FEDER Funds through Project CTQ2013-41,354-R, and from Gobierno de Extremadura and FSE Funds through Project RNM021. E. Rodriguez thanks the Gobierno de Extremadura and FSE Funds for her FPI PhD Grant.

References

[1] N. Bolong, A.F. Ismail, M.R. Salim, T. Matsuura, A review of the effects of emerging contaminants in wastewater and options for their removal, Desalination 239 (2009) 229–246.

[2] K. Ikehata, M.G. El-Din, S.A. Snyder, Ozonation and advanced oxidation treatment of emerging organic

pollutants in water and wastewater, Ozone Sci. Eng. 30 (2008) 21–26.

[3] L. Kovalova, H. Siegrist, U. von Gunten, J. Eugster, M. Hagenbuch, A. Wittmer, R. Moser, C.S. McArdell, Elimination of micropollutants during post-treatment of hospital wastewater with powdered activated carbon, ozone, and UV, Environ. Sci. Technol. 47 (2013) 7899–7908.

[4] N. Nakada, K. Komori, Y. Suzuki, C. Konishi, I. Houwa, H. Tanaka, Occurrence of 70 pharmaceutical and personal care products in Tone River basin in Japan, Water Sci. Technol. 56 (2007) 133–140.

[5] P. Westerhoff, Y. Yoon, S. Snyder, E. Wert, Fate of endocrine-disruptor, pharmaceutical, and personal care product chemicals during simulated drinking water treatment processes, Environ. Sci. Technol. 39 (2005) 6649–6663.

[6] P.E. Stackelberg, E.T. Furlong, M.T. Meyer, S.D. Zaugg, A.K. Henderson, D.B. Reissman, Persistence of pharmaceutical compounds and other organic wastewater contaminants in a conventional drinking-water-treatment plant, Sci. Total Environ. 329 (2004) 99–113.

[7] U. Goren, A. Aharoni, M. Kummel, R. Messalen, I. Mukmenev, A. Brenner, V. Gitis, Role of membrane pore size in tertiary flocculation/adsorption/ultrafiltration treatment of municipal wastewater, Sep. Purif. Technol. 61 (2008) 193–203.

[8] N.M. Al-Bastaki, Performance of advanced methods for treatment of wastewater: UV/TiO_2, RO and UF, Chem. Eng. Process. 43 (2004) 935–940.

[9] T. Wintgens, T. Melin, A. Schafer, S. Khan, S. Muston, D. Bixio, C. Thoeye, The role of membrane processes in municipal wastewater reclamation and reuse, Desalination 178 (2005) 1–11.

[10] A.R.D. Verliefde, S.G.J. Heijman, E.R. Cornelissen, G. Amy, B. Van der Bruggen, J.C. van Dijk, Influence of electrostatic interactions on the rejection with NF and assessment of the removal efficiency during NF/GAC treatment of pharmaceutically active compounds, Water Res. 41 (2007) 3227–3240.

[11] J. Haberkamp, M. Ernst, U. Bockelmann, U. Szewzyk, M. Jekel, Complexity of ultrafiltration membrane fouling caused by macromolecular dissolved organic compounds in secondary effluents, Water Res. 42 (2008) 3153–3161.

[12] H.E. Wray, R.C. Andrews, P.R. Bérubé, Surface shear stress and retention of emerging contaminants during ultrafiltration for drinking water treatment, Sep. Purif. Technol. 122 (2014) 183–191.

[13] A.H.M. Anwar Sadmani, R.C. Andrews, D.M. Bagley, Nanofiltration of pharmaceutically active compounds as a function of compound interactions with DOM fractions and cations in natural water, Sep. Purif. Technol. 122 (2014) 462–471.

[14] P.A. Neale, A.I. Schafer, Quantification of solute-solute interactions in steroidal hormone removal by ultrafiltration membranes, Sep. Purif. Technol. 90 (2012) 31–38.

[15] E.-E. Chang, U.-C. Chang, C.-H. Liang, C.-P. Huang, P.-C. Chiang, Identifying the rejection mechanism for nanofiltration membranes fouled by humic acids and calcium ions exemplified by acetaminophen, sulfamethoxazole, and triclosan, J. Hazard. Mater. 221–222 (2012) 19–27.

[16] C. Bellona, J.E. Drewes, P. Xu, G. Amy, Factors affecting the rejection of organic solutes during NF/RO treatment—A literature review, Water Res. 38 (2004) 2795–2809.

[17] L.D. Nghiem, A.I. Schafer, M. Elimelech, Pharmaceutical retention mechanisms by nanofiltration membranes, Environ. Sci. Technol. 39 (2005) 7698–7705.

[18] L.D. Nghiem, S. Hawkes, Effects of membrane fouling on the nanofiltration of pharmaceutically active compounds (PhACs): Mechanisms and role of membrane pore size, Sep. Purif. Technol. 57 (2007) 176–184.

[19] A.I. Schafer, L.D. Nghiem, A. Meier, P.A. Neale, Impact of organic matrix compounds on the retention of steroid hormone estrone by a 'loose' nanofiltration membrane, Sep. Purif. Technol. 73 (2010) 179–187.

[20] A.M. Comerton, R.C. Andrews, D.M. Bagley, The influence of natural organic matter and cations on the rejection of endocrine disrupting and pharmaceutically active compounds by nanofiltration, Water Res. 43 (2009) 613–622.

[21] A.M. Comerton, R.C. Andrews, D.M. Bagley, C. Hao, The rejection of endocrine disrupting and pharmaceutically active compounds by NF and RO membranes as a function of compound and water matrix properties, J. Membr. Sci. 313 (2008) 323–335.

[22] T. Fujioka, L.D. Nghiem, S.J. Khan, J.A. McDonald, Y. Poussade, J.E. Drewes, Effects of feed solution characteristics on the rejection of N-nitrosamines by reverse osmosis membranes, J. Membr. Sci. 409–410 (2012) 66–74.

[23] R. Loos, B.M. Gawlik, G. Locoro, E. Rimaviciute, S. Contini, G. Bidoglio, EU wide survey of polar organic persistent pollutants in European river waters, Environ. Pollut. 157 (2009) 561–568.

[24] S.D. Costanzo, A.J. Watkinson, E.J. Murby, D.W. Kolpin, M.W. Sandstrom, Is there a risk associated with the insect repellent DEET (N, N-diethyl-m-toluamide) commonly found in aquatic environments? Sci. Total Environ. 384 (2007) 214–220.

[25] W. Boehmer, H. Ruedel, A. Wenzel, C. Schröeter-Kermani, Retrospective monitoring of triclosan and methyl-triclosan in fish: Results from the german environmental specimen bank, Organohalogen Compd. 66 (2004) 1489–1494.

[26] L. Wenhui, L. Xinghai, L. Dongyan, S. Lei, S. Qi, Vapor-phase synthesis of 3-methylindole over Fe-, Co-, or Ni-promoted Ag/SiO_2, Chin. J. Catal. 30 (2009) 1287–1290.

[27] K.H. Langford, K.V. Thomas, Determination of pharmaceutical compounds in hospital effluents and their contribution to wastewater treatment works, Environ. Int. 35 (2009) 766–770.

[28] L.S. Clesceri, A.E. Greenberg, R.R. Trussell, Standard Methods for the Examination of Water and Wastewater, seventeenth ed., APHA, AWWA, WPCF, Washington, DC, 1989.

[29] F.J. Benitez, J.L. Acero, F.J. Real, G. Roldan, E. Rodriguez, Photolysis of model emerging contaminants in ultra-pure water: Kinetics, by-products formation and degradation pathways, Water Res. 47 (2013) 870–880.

[30] J.L. Acero, F.J. Benitez, A.I. Leal, F.J. Real, F. Teva, Membrane filtration technologies applied to municipal

secondary effluents for potential reuse, J. Hazard. Mater. 177 (2010) 390–398.

[31] Y. Yoon, P. Westerhoff, S.A. Snyder, E.C. Wert, Nanofiltration and ultrafiltration of endocrine disrupting compounds, pharmaceuticals and personal care products, J. Membr. Sci. 270 (2006) 88–100.

[32] N. Maximous, G. Nakhla, W. Wan, Comparative assessment of hydrophilic membrane fouling in wastewater applications, J. Membr. Sci. 339 (2009) 93–99.

[33] L.D. Nghiem, P.J. Coleman, C. Espendiller, Mechanisms underlying the effects of membrane fouling on the nanofiltration of trace organic contaminants, Desalination 250 (2010) 682–687.

[34] A. Altapova, E.-S. Kim, S. Dong, N. Sun, P. Chelme-Ayala, M.G. El-Din, Treatment of oil sands process-affected water with ceramic ultrafiltration membrane: Effects of operating conditions on membrane performance, Sep. Purif. Technol. 122 (2014) 170–182.

[35] M.R. Teixeira, M.J. Rosa, Microcystins removal by nanofiltration membranes, Sep. Purif. Technol. 46 (2005) 192–201.

[36] M.J. López-Muñoz, A. Sotto, J.M. Arsuaga, B. Van der Bruggen, Influence of membrane, solute and solution properties on the retention of phenolic compounds in aqueous solution by nanofiltration membranes, Sep. Purif. Technol. 66 (2009) 194–201.

[37] M.R. Teixeira, M.J. Rosa, M. Nystrom, The role of membrane charge on nanofiltration, J. Membr. Sci. 265 (2005) 160–166.

[38] B. Van der Bruggen, J. Shaep, W. Maes, D. Wilms, C. Vandecasteele, Nanofiltration as a treatment method for the removal of pesticides from ground waters, Desalination 117 (1998) 139–147.

[39] K. Katsoufidou, S.G. Yiantsios, A.J. Karabelas, A study of ultrafiltration membrane fouling by humic acids and flux recovery by backwashing: Experiments and modelling, J. Membr. Sci. 266 (2005) 40–50.

[40] F.J. Benitez, J.L. Acero, F.J. Real, C. Garcia, Combination of chemical oxidation-membrane filtration processes for the elimination of phenyl-ureas in water matrices, J. Chem. Technol. Biotechnol. 84 (2009) 1883–1893.

[41] Q. Li, M. Elimelech, Organic fouling and chemical cleaning of nanofiltration membranes: Measurements and mechanisms, Environ. Sci. Technol. 38 (2004) 4683–4693.